PLANT SCIENCE TODAY
Vol XX(1): 1-XX
https://doi.org/10.14719/pst.16217

eISSN 2348-1900
OPEN ACCESS

Research Article | Pharmacology
2026, Volume XX, Issue X, pp. 1-XX

Bioactive phytochemical extraction and characterisation from *Solanum nigrum*: an investigation of antirabies compounds using an *in silico* approach

Pulamai Dasan Perumal & N P M Mohamed Tariq*

Post Graduate and Research Department of Biotechnology, Islamiah College (Autonomous) (Affiliated to Thiruvalluvar University), Vaniyambadi 635 752, Tamil Nadu, India

***Correspondence:** npmtariq@gmail.com

Abstract

The present study includes the phytochemical evaluation of *Solanum nigrum* methanol extract; 1.64 % (0.82 g), revealing an 80 % positive detection rate for major phytochemical tests. The column-eluted fractions obtained by methanol and hexane solvents were efficient in separating the compounds with a ratio of 3 : 7 and 2 : 8 respectively. The gas chromatography mass spectrometry study of the collected fractions showed the presence of 19 different compounds from a total of 30 peaks. Major compounds identified included 3,3-dimethylpiperidine, 3-methylhexan-2-amine, N-dl-Alanylglycine, (S)-(+)-1-cyclohexylethylamine, tetratriacontane, lauramide, piperazine, amino acids and their derivatives. A bioassay of the extract for 2,2-diphenyl-2-picryl hydrazyl scavenging showed concentration-dependent activity, recording a maximum of 68.041 % and anti-inflammatory activity of 67.4 % at 100 µg/mL. The 3D structural study of the targeted rabies virus glycoprotein revealed that the G-chain contained a cavity volume of 65.4 Å^3 without any tunnels, implying a low transportability function. Chain A was found to have a relatively high pocket volume of 565.1 Å^3 along with one or several tunnels, which indicates the existence of significant ligand binding sites. Docking against G-chain revealed that N-dl-Alanylglycine had the highest binding affinity with a docking score of −4.86 kcal/mol. On the other hand, docking against Chain A indicated that lauramide is the most effective compound among the two, with a docking score of −5.583 kcal/mol. The binding affinities of the selected molecules revealed that both could inhibit the binding capacity of the virus during infection. The current results indicate that the selection of candidates and the hypothesis supporting the effectiveness of phytocompounds against rabies might require additional exploration through *in vivo* research.

Keywords: anti-rabies; docking; dodecanamide; dipeptide; glycoprotein; *Solanum* sp

Received: 19 June 2026. **Accepted:** 18 October 2026. **Available online:** Version 1.0: 19 November 2026.

Cite this article: Pulamai DP, Mohamed NPMT. Bioactive phytochemical extraction and characterisation from *Solanum nigrum*: an investigation of antirabies compounds using an *in silico* approach. Plant Science Today. 2026;XX(X):1-XX. https://doi.org/10.14719/pst.16217

Introduction

The rabies virus causes an acute encephalitic disease known as rabies. The prototype rabies virus belongs to the *Rhabdoviridae* family. Rabies is a preventable viral disease that mostly affects mammals and is spread by the bite of rabid animals, which contaminates an afflicted animal's saliva. Once symptoms appear, rabies has no cure; however, vaccination offers protection against the disease. Several studies in the country have evaluated the efficacy of certain ethnomedical and traditional herbs against rabies through modern pharmacological methods (1). Before the development of modern health sciences, cultures used herbal medicine as a form of ancient medicine. Indigenous theories, beliefs and experiences have been passed down through the years, forming the foundation of traditional medicine (2). Several Asian nations have recognised the necessity and significance of creating improved traditional medicines (ITM) from native and endemic plants that have historically been utilised for a variety of viral infections (3, 4). Pharmaceutical companies have a lasting interest in medicinal substances obtained from plant extracts. For instance, taxol is an anticancer medication derived from the bark of the western yew tree, recognised for its effectiveness in treating breast cancer. The *Solanum* group of plants is a vast genus within the Solanaceae family, comprising nearly 2000 species that include both food plants and medicinal herbs (5). The genus *Solanum* has garnered significant attention in both chemical and biological research during the past 30 years. Multiple steroidal saponins, steroidal alkaloids, disaccharides, flavonoids and phenolic compounds have been associated with biological activities and tumour growth inhibition (6–8). The *Solanum* genus is the most extensive in the Solanaceae family, commonly referred to as nightshades, consisting of about 85–90 genera distributed in tropical and subtropical regions (9). Extracts from this herb have

been reported to mitigate cytotoxicity, hepatotoxicity and support organ health due to the presence of medicinally important alkaloids. *Solanum nigrum* L. compounds have strong antibacterial, anti-inflammatory, anti-diabetic and immunostimulant effects and have also proven anti-cancer effects. The presence of numerous phytochemicals makes this plant possibly a valuable and potent plant with the best outcomes in pharmacological tests. Solanaceae species also possess toxic alkaloids that can cause effects in humans and animals, from mild irritation to lethal consequences (10). Therefore, this study aims to partially purify compounds from *S. nigrum* to evaluate its chemical profile and effectiveness as an antiviral drug.

Materials and Methods

Plant material collection and extract preparation

Solanum nigrum was collected from the area of Peddur village, Alangayam town, Tirupattur district, Tamil Nadu, India (Fig. 1). Leaf samples were washed with distilled water and dried at room temperature in the shade. The dried leaf samples were ground using a laboratory mill and sieved. The fine powdered sample (10 g) was dissolved and agitated in methanol (100 mL) for 4 days. The solvent phase was collected by filtration, then concentrated using a rotary evaporator at 50 °C until all the solvent evaporated.

Column chromatography with gradient solvent elution technique

Column chromatography was done to isolate the plant constituents from the crude extract. A portion of 5 g of dried extract was first dissolved using a minimal amount of solvent used and then loaded on the silica gel column (8 cm) packed with 60–120 mesh and pre-equilibrated hexane. Careful loading of the extract was made and allowed adsorption on the solid phase in preparation for the elution process. The extract was isolated using a gradient solvent system which had an increasing level of polarity. Initially, elution was carried out using the solvent hexane (A1), followed by the A2 gradient containing hexane : ethylacetate (9 : 1, 5 : 5 and 1 : 9). Further A3 hexane-methanol (7 : 3 ratio), A4 methanol hexane (7 : 3) and hexane-ethyl acetate-methanol (2 : 1 : 1) were applied and the elution was then continued. The R_f values of fractions examined for homogeneity using the thin-layer chromatography (TLC) method and similar retention factor components were collected for gas chromatography–mass spectrometry (GCMS).

Phytochemical studies

Mayer's test for alkaloid

Two millilitres of the extract were treated with several drops of Mayer's reagent (11). The precipitation that occurs in the form of a cream or pale yellow colour indicates the presence of alkaloids.

Carbohydrates (Molisch's test)

One part of the leaf extract was combined with a few drops of Molisch's reagent. Then, 1 mL of concentrated sulfuric acid was gradually added to the mixture alongside the tube. A violet or purple ring that forms at the interface confirms the presence of carbohydrates.

Glycosides (Keller-Killiani test)

Equal volumes of extract were combined with 2 mL of glacial acetic acid containing ferric chloride solution. This mixture was then combined with concentrated sulfuric acid in the test tube. Formation of a brown ring at the boundary between the two solutions indicates cardiac glycosides.

Saponins test

A dilution of 1 mL of the extract in 5 mL of distilled water was prepared in a 15 mL test tube and vigorously mixed 3 times to give rise to a permanent froth of at least 1 cm in height. Stable foam indicates a positive test.

Proteins (Biuret test)

A reaction between 2 mL of the extract and 1 mL of 10 % sodium hydroxide solution, together with a few drops of 0.1 % copper sulfate solution, was carried out. Formation of a purple or violet colored solution confirms the presence of protein.

Amino acids (ninhydrin test)

To 0.5 mL of extract diluted with 0.5 mL water, a few drops of 0.2 % ninhydrin reagent were added. The sample mixture tube was boiled in a water bath for 5 min. A reaction with the production of purple or blue colouring was an indication of the presence of amino acids.

Phenolic compounds (ferric chloride test)

Two millilitres of the extract were treated with a few drops of 5 % ferric chloride solution. The presence of phenolic compounds was confirmed by the appearance of blue or black colouring.

Flavonoids (alkaline reagent test)

The plant extract was combined with a few drops of 10 % sodium hydroxide solution. The appearance of an intensely colored yellow substance that disappeared when hydrochloric acid was added indicated the presence of flavonoids.

Terpenoids (Salkowski test)

Equal volume of the extract was dissolved in chloroform and subsequently, 1 mL of conc. sulphuric acid was added carefully down the side of the test tube. The formation of a reddish-brown colouration was an indication that terpenoids were present.

Steroids (Liebermann-Burchard test)

Two millilitres of the extract were dissolved in 2 mL chloroform, then treated with 2 mL of acetic anhydride and a few drops of concentrated sulphuric acid (H_2SO_4). The emergence of a blue-green colour was an indication that there were steroids present.

© The Author(s) 2026. Creative Commons CC BY 4.0. Published by Horizon e-Publishing Group.
https://doi.org/10.14719/pst.16217



Fig. 1. Sampling site and authentication of *Solanum nigrum.*

Thin layer chromatography of *Solanum nigrum* (leaf)

Thin-layer chromatography analysis of the column-eluted fractions was carried out. The TLC plates were prepared using silica gel G and activated at 110 °C for 1 hr. Sample fractions were applied to the TLC plates as spots using glass capillary tubes and allowed to develop in the saturated chromatographic chamber at room temperature. Several solvent systems were used to obtain better separation of the compounds. Hexane, ethyl acetate and methanol were found to be suitable solvent systems for better separation of compounds. The developed TLC plates were dried with air and visualised under UV and visible light. The values of the retention factor (R_f) for the spotted fractions were determined and similar fractions were collected.

Compound analysis by GC–MS

The collected column fractions chemical profile was analysed by GC–MS analysis. The analysis was done using a GC–MS-QP2010 Plus Shimadzu coupled with the AOC-20i auto-injector system. The plant extract sample, after filtration through a 0.22 µm syringe filter, was concentrated using a rotary evaporator at reduced pressure and later dissolved in High-performance liquid chromatography (HPLC) grade methanol. A capillary column with Rxi-5Sil MS was employed for sample separation. The column dimensions were 30 m length, 0.25 mm internal diameter and 0.25 µm film thickness. Helium (≥ 99.999 % purity) was used as the carrier gas with a constant flow rate of 1.0 mL/min. The injector was maintained at a constant temperature of 250 °C with a split ratio of 10 : 1. Oven temperature programming started from an initial temperature of 60 °C, which was held for 2 min and increased at the rate of 10 °C/min to a final temperature of 280 °C, which was held for 10 min. The leaf extract sample was analysed under EI conditions at 70 eV for mass spectrometric detection. Ion source temperature and interface temperature were maintained at 200 °C and 250 °C respectively. Mass spectra were recorded in the range of m/z 40–600. Chromatograms and mass spectra were analysed using Shimadzu GC–MS solution software with NIST (National Institute of Standards and Technology) library database.

2, 2 Diphenyl-2-picryl hydrazyl (DPPH) radical scavenging assay

The partially purified plant extract was subjected to the DPPH method for the free radical scavenging assay (12). The known concentration of test samples (25 to 100 µg) was combined in various concentrations with 100 µL of a DPPH solution made in methanol (40 mM) in 1 mL total volume. The combination was incubated for 30 min at room temperature and in the dark to produce the desired colour, which was measured at 517 nm along with ascorbic acid as a standard. Each sample's DPPH scavenging activity was estimated using the formula below

$$\text{Scavenging activity (\%)} = 100 \times (Ac - At)/Ac$$

Where At is the absorbance of the test sample and Ac is the absorbance of the control reaction (100 µL of methanol and 100 µL of DPPH solution).

In vitro anti-inflammatory egg albumin denaturation test

For the evaluation of the anti-inflammatory activity, the egg albumin denaturation test was employed with minor changes (13). The reaction mixture (5 mL) contained 1 mL of egg albumin, 3 mL of phosphate-buffered saline

© The Author(s) 2026. Creative Commons CC BY 4.0. Published by Horizon e-Publishing Group.
https://doi.org/10.14719/pst.16217

(PBS; pH 6.4) and 1 mL of sample or standard drug in varying concentrations (20, 40, 60, 80 and 100 µg/mL). Another set of mixtures without the sample but instead with PBS was also prepared to serve as controls. These were incubated at 37 °C for 15 min, followed by heating at 70 °C for 10 min. The absorbances were determined at 600 nm against the blank and the inhibition rate of protein denaturation was computed using standard diclofenac with the equation below :

$$\% \text{ Inhibition} = ((Ac - At) / Ac) \times 100$$

where Ac = absorbance of control and At = absorbance of test sample

Molecular docking

The three-dimensional crystal structure of the rabies glycoprotein was obtained from the Protein Data Bank (*PDB* ID : 6TOU). AutoDock was used to generate the protein structure by removing water molecules, heteroatoms and co-crystallised ligands. RondonQSAR was used for ligand evaluation. Prank was used to find pockets and tunnels of the receptor using AlphaFold conservation. The protein received Kollman charges and polar hydrogen atoms were introduced. Once prepared, the structure was stored in the PDB, partial charge and atom type (PDBQT) format for docking studies. The chemical structures of ligands (lauramide, N-dl-alanylglycine and ribavirin) were retrieved from the PubChem database. Chem3D was utilised to lower the energy of the ligand structure and it was subsequently converted to *PDB* format. AutoDock Tools were utilised for additional preparation, which involved adding hydrogen atoms and assigning Gasteiger charges. The ligand was converted into MOL2 format. Then, AutoDock Vina was used to assess interactions with the target receptor through molecular docking. To perform the docking, a grid box was created at the active site, setting the right dimensions and central coordinates (14).

Results and discussion

Phytochemical profiling

The collected sample, identified at the Rapinat Herbarium and Centre for Molecular Systematics, St. Joseph's College (Autonomous), Tiruchirappalli, was authenticated with voucher number PPD 002. The qualitative analysis of the leaf extract of *S. nigrum* showed positive results for 8 out of the 10 tests (Table 1). Methanol extraction yielded 1.64 % (0.82 g), which indicated the presence of alkaloids, flavonoids, steroids, phenolics, glycosides, saponins, amino acids and proteins in the plant. Carbohydrates and terpenoids were not detected. *Solanum nigrum* is regarded as having a diverse phytochemical profile (5). The presence of alkaloids exhibits antimicrobial, anticancer and anti-inflammatory activities, while phenols and flavonoids are noted for their powerful antioxidant activity (15). Steroidal glycoalkaloids represent the most prevalent and significant category of nitrogenous secondary metabolites found in plants of the Solanaceae family (16).

Different types of solvent systems with different gradients were employed in TLC for the separation of phytoconstituents in the extract (Table 2). Of the different solvent systems, hexane alone gave rise to only one fraction (R_f 0.025). The separation ability was further improved in the hexane-ethyl acetate mixture with 1 : 9 ratios that could separate out 3 fractions (R_f 0.052). There was inconsistency in the efficiency of separation using the hexane-methanol solvent system. However, a 6: 4 ratio (A3.4) could separate 5 fractions, thus making the process efficient. A similar better chromatogram resolution was observed with methanol-hexane mixture (3 : 7 and 2 : 8 ratio) had 5 and 6 distinct bands, respectively with R_f values of 0.025 to 0.325. In the triple solvent mixture of hexane, ethyl acetate and methanol, the solvent mixture in the ratio of 6 : 3 : 1 (A5.2) resulted in 3 separated fractions, indicating fair resolution power. In general, the solvent mixture of methanol-hexane (2 : 8) was the most efficient solvent system for the separation, with the next being that of hexane-methanol (4 : 6). From the data above, it is clear that the polarity of the solvent plays a crucial role in compound separation and the most effective solvent mixture for separation was that of methanol-hexane in a ratio of 2 : 8. Polar and semi-polar solvents improve the resolution of bioactive compounds by increasing the interaction with the stationary and mobile phases (17). Thin layer chromatography does not give as precise quantitative values as HPLC, but it may serve as an auxiliary method for estimation of the percentage of active substances. This technique helped rapidly assess the crude extract during partial purification (18).

GC–MS analysis of extract fractions

The GC–MS analysis of the extract shows that 19 compounds from 30 peaks were identified in the range of retention time from 7.513 to 38.590 min, totalling a peak area of 3633025 (Fig. 2, Table 3). The identified peaks were mostly made up of amines, amino acid derivatives, hydrocarbons and amides. Tetratriacontane was found to be one of the major peaks in the sample, at retention times of 36.075, 37.356 and 38.590 min. Several compounds, including N-dl-alanylglycine, (S)-(+)- 1-cyclohexylethylamine and tetratriacontane, appeared at multiple retention times. Some other prominent peaks include hentriacontane, 3,3-dimethylpiperidine, D-alanine, N-dl-alanylglycine and (S)-(+)-1-Cyclohexylethylamine. Amino acid derivatives, including D-alanine, alanylglycine, dl-Alanyl-dl-valine and dl-Alanyl-dl-α-amino-n-butyric acid, were detected at multiple retention times, reflecting the chemical complexity of the sample. In addition, lauramide, N-(2-phenylethyl)-N-methyl- and pentanoic acid, 5-hydroxy-, 2,4-di-tert-butylphenyl ester were identified as minor constituents.

© The Author(s) 2026. Creative Commons CC BY 4.0. Published by Horizon e-Publishing Group.
https://doi.org/10.14719/pst.16217

Table 1. Preliminary phytochemical analysis of the leaf extract of *Solanum nigrum*

Sl. no	Phytochemical test	Presence of phytochemical compounds differentiated by colour	Results
1.	Alkaloids	A precipitate with reddish-brown colour	+
2.	Carbohydrates	A red colour indication	-
3.	Glycosides	Pink colour indication	+
4.	Saponins	Foam persists indication	+
5.	Proteins	The formation of a purplish-violet colour	+
6.	Amino acids	Purple colour indication	+
7.	Phenolic compounds	A dark green color indication	+
8.	Flavonoids	Yellowish color formation	+
9.	Terpenoids	To form a reddish brown layer	-
10.	Steroids	Blue and green color indications	+

Table 2. Fractions collected through column eluted extract

Solvent	Gradient	No. of visible fraction	R_f value
A1	Hexane	1	0.025
A2	Hexane –ethyl acetate		
	(9 : 1)	1	0.034
	(5 : 5)	1	0.025
	(1 : 9)	3	0.052, 0.034, 0.025
A3	Hexane-methanol		
A3.1	9 : 1	4	0.03, 0.310, 0.032, 0.034
A3.2	8 : 2	3	0.04, 0.25, 0.033
A3.3	6 : 4	5	0.06, 0.25, 0.035, 0.36,0.42
A3.4	4 : 6	3	0.05, 0.027, 0.045
A3.5	3 : 7	2	0.03, 0.02
A3.6	2 : 8	2	0.05, 0.036
A3.7	1 : 9	1	0.05
A4	Methanol - hexane		
A4.1	9 : 1	2	0.01, 0.001
A4.2	8 : 2	3	0.025,0.02, 002
A4.3	6 : 4	3	0.052, 0.21,0.025
A4.4	4 : 6	3	0.05, 0.025, 0.027
A4.5	3 : 7	5	0.05, 0.04, 0.03, 0.025, 0.027
A4.6	2 : 8	6	0.05, 0.036, 0.027, 0.025 0.045, 0.01
A4.7	1 : 9	2	0.05, 0.25
A5	Hexane-ethyl acetate-methanol		
A5.1	7 : 2 : 1	2	0.025,0.01
A5.2	6 : 3 : 1	3	0.05, 0.032, 0.023

© The Author(s) 2026. Creative Commons CC BY 4.0. Published by Horizon e-Publishing Group.
https://doi.org/10.14719/pst.16217

Table 3. NIST matched compound related to GC–MS peak

Peak#	Retention time	Area %	NIST identity %	Compound Name
1	7.513	196012	85	3,3-dimethylpiperidine
2	10.120	176645	85	Piperazine, 2-methyl-
3	12.314	84624	80	(Cyclohexylmethyl)(methyl)amine
4	12.693	46149	89	1-methyldecylamine
5	18.840	21338	86	3-methylhexan-2-amine
6	18.901	6419	90	3-methylhexan-2-amine
7	19.054	23823	85	D-alanine
8	19.781	107571	73	Pentanoic acid, 5-hydroxy-, 2,4-di-t-butylphen
9	22.324	188949	69	D-alanine
10	23.643	20910	88	N-dl-alanylglycine
11	25.184	49715	82	N-dl-alanylglycine
12	26.094	84154	82	(2-Cyclohexylpropyl)(methyl)amine
13	26.835	28133	88	(S)-(+)-1-Cyclohexylethylamine
14	26.945	15753	89	2-Butanamine, 3,3-dimethyl-
15	27.220	77878	79	(S)-(+)-1-Cyclohexylethylamine
16	27.585	18759	87	dl-alanyl-dl-valine
17	27.757	25909	88	N-dl-alanylglycine
18	28.052	33024	83	(S)-(+)-1-cyclohexylethylamine
19	30.730	33488	89	N-dl-alanylglycine
20	30.865	58158	78	dl-alanyl-dl-.alpha.-amino-n-butyric acid
21	31.920	32031	86	N-dl-alanylglycine
22	33.360	118013	80	3,3-dimethylpiperidine
23	34.744	258203	85	Hentriacontane
24	36.075	529578	89	Tetratriacontane
25	36.131	73291	77	Lauramide, N-(2-phenylethyl)-N-methyl-
26	37.356	632785	89	Tetratriacontane
27	38.024	29270	80	N-dl-alanylglycine
28	38.126	30915	79	N-dl-alanylglycine
29	38.256	24459	79	N-dl-alanylglycine
30	38.590	619905	88	Tetratriacontane
Total		3633025		

© The Author(s) 2026. Creative Commons CC BY 4.0. Published by Horizon e-Publishing Group.
https://doi.org/10.14719/pst.16217

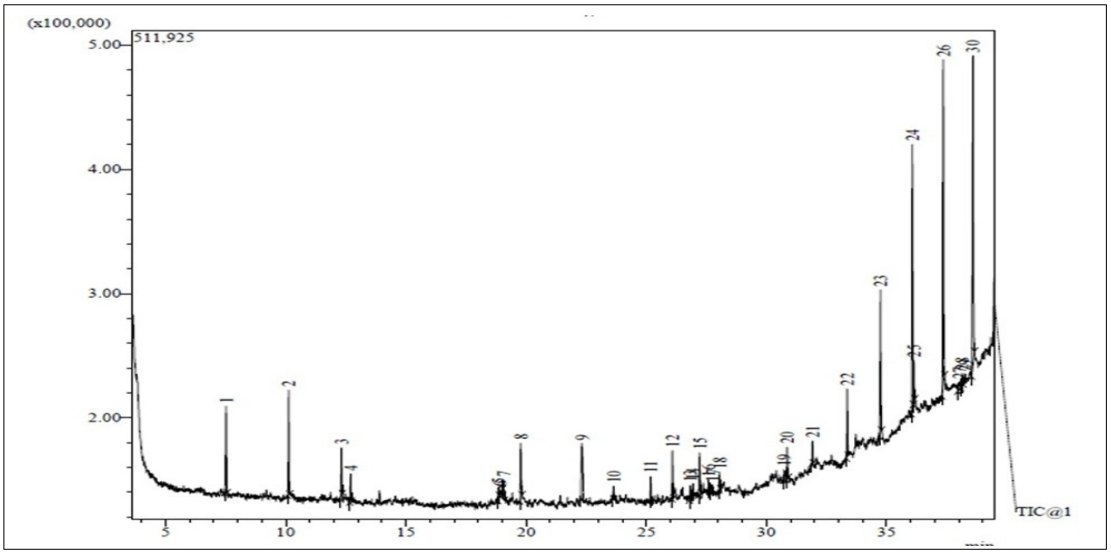


Fig. 2. GC−MS Spectrum of collected fraction pool.

The identification of hentriacontane, peaking at 34.744 min with an area of 258203, further confirms the presence of bioactive hydrocarbons in *S. nigrum* (Table 3). Long-chain hydrocarbons like tetratriacontane and hentriacontane are commonly found in medicinal plants and are well-known for their antioxidant, antimicrobial and anti-inflammatory responses in plants (19). Several aliphatic and cyclic amines such as 3-methylhexan-2-amine,1-methyldecylamine, cyclohexylmethylamine and 2-cyclohexylpropylamine suggest the presence of the alkaloid class (20). Detection of peptides and amino acid derivatives suggests biologically active metabolites playing an important role in the physiological process and might have antioxidant functions. Another component found is lauramide, N-(2-phenylethyl)-N-methyl-, a derivative of a fatty acid amide, which exhibits surface activity and biological activity. Pentanoic acid, 5-hydroxy-, 2,4-di-t-butylphenyl ester was another compound that was determined and could exhibit antioxidant properties owing to the phenol-like structure present in this compound. The dominance of hydrocarbons, alkaloids, amines, amino acid derivatives and fatty acids highlights the diverse chemical composition of the chromatography fractions (21).

Biological significance of *Solanum nigrum* extract

The free radical scavenging ability of the methanolic leaf extract of *S. nigrum* was assessed by DPPH free radical scavenging method and compared with the known antioxidant ascorbic acid (Fig. 3). The methanolic extract showed concentration dependent free radical scavenging properties with inhibition values ranging from 20.77 ± 0.54 % for 20 µg/ml and steadily increased as 41.96 ± 0.34, 57.99 ± 0.26, 62.25 ± 0.56 among and the maximum of 68.05 ± 0.21 % was recorded in 100 µg/ml with IC_{50} 40.131 ± 4.7 (R^2 0.99685). The inhibition percentage recorded for ascorbic acid was 17.33 ± 1.1, 41.16 ± 1.0, 65.66 ± 0.5, 77.66 ± 0.5, 80.66 ± 1.15 across 20 to 100 µg, with an IC_{50} of 45.57366 ± 0.9 µg (R^2 0.99971) (Table 4). The free radical scavenging of the extract was attributed to high levels of polyphenols, flavonoids and other phytochemicals in the plant (22). Aqueous extract alone significantly restrained stress-induced oxidative stress in rats (23).

The anti-inflammatory activity of *S. nigrum* leaves was studied against diclofenac sodium at different concentrations. There was a dose response relationship of protein denaturation inhibition recorded at 11.10 ± 0.84 to 31.72 ± 0.55 to 67.42 ± 0.10 % activity (Fig. 4). The activities of diclofenac sodium were recorded as 17 ± 1.73, 32 ± 5.29, 56.66 ± 2.3094, 68.66 ± 1.15 and 82.4 ± 0.4 respectively. Statistical significance among mean values was determined using a one-way ANOVA (p < 0.0001 and F value 427.60391). The IC_{50} by nonlinear regression fit was 68.02 (R^2 0.9996) for the extract and 61.90 µg (R^2 0.9956) for the standard drug, suggesting the presence of plant bioactive compounds with good anti-inflammatory properties. Previous research has shown that the plant *S. nigrum* has considerable anti-inflammatory properties because of the presence of steroidal alkaloids, flavonoids and phenolics in it (24).

In silico analysis of identified phytocompounds

Pocket analysis of rabies glycoprotein G chain

The analysis of the pocket of the rabies glycoprotein showed one binding pocket with a volume of 65.4 Å³. The identified binding pocket corresponds to a relatively small surface pocket, which could be used as a target site for a docking interaction for antiviral drugs (Fig. 5). Protein pockets are critical for forming connections between a protein and small molecules, peptides and other biological compounds. No tunnels were found within the analysed structure of the rabies glycoprotein. The lack of tunnels means that there are no continuous channels leading from the binding pocket to the protein surface (25). The presence of binding sites without tunnels confirms that the protein does not have the ability to transport any substances. The relatively small binding pocket volume (65.4 Å³) shows the existence of a small pocket, where only small ligands or certain amino acid residues can interact (26).

© The Author(s) 2026. Creative Commons CC BY 4.0. Published by Horizon e-Publishing Group.
https://doi.org/10.14719/pst.16217

Table 4. Descriptive statistics on DPPH assay

Sample	N Analysis	N Missing	Mean	Standard deviation	SE of Mean
Ext 20	3	0	20.77	0.5	0.30905
Ext 40	3	0	41.96	0.3	0.2
Ext 60	3	0	57.99	0.2	0.15275
Ext 80	3	0	62.25	0.5	0.32604
Ext 100	3	0	68.04	0.2	0.12129
Std 20	3	0	17.33	1.1	0.66667
Std 40	3	0	41.16	1.0	0.60093
Std 60	3	0	65.66	0.5	0.33333
Std 80	3	0	77.66	0.5	0.33333
Std 100	3	0	80.66	1.15	0.66667
P value		<0.0001			
F Value		2817.3138			

Ext: Extract; std: Standard.

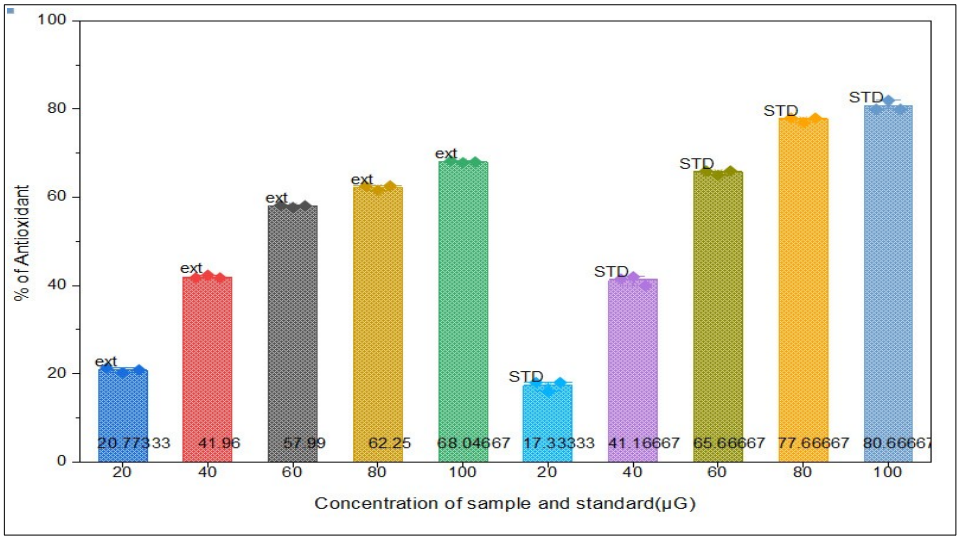


Fig. 3. Percentage of DPPH scavenging activity of extract and standard.

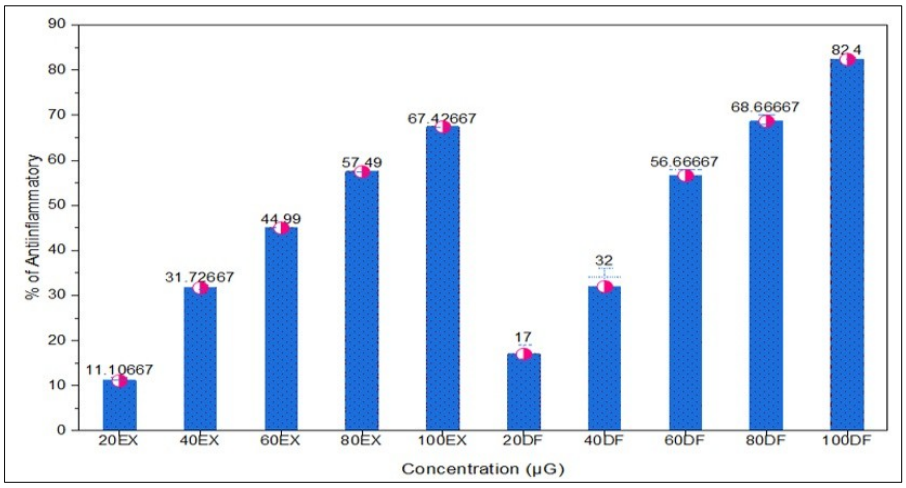


Fig. 4. Percentage of albumin denaturation inhibition by extract and standard.

© The Author(s) 2026. Creative Commons CC BY 4.0. Published by Horizon e-Publishing Group.
https://doi.org/10.14719/pst.16217

Pocket and tunnel analysis of rabies glycoprotein chain A

Based on the structural analysis of rabies glycoprotein Chain A, it was observed that there is an active binding pocket with a volume of 565.1 Å³ (Fig. 6a). As compared to small surface pockets, this pocket appears to be large and accessible, which means that it might bind multiple molecules to interact with different types of molecules. The presence of a large pocket indicates the presence of major active or allosteric sites where drugs may be developed based on their structures. Cavities such as this one usually represent a part of protein-protein interactions, ligand/receptor interactions and binding processes that take place during viral entry into the host cell.

The tunnel analysis indicated that there was one or more surface-accessible tunnels present in connection with the binding pocket (Fig. 6b). Tunnels play an important role in enabling the movement of molecules from the protein surface to the protein interior binding site. This tunnel might enable the access of ligands to the binding pocket. This tunnel could make it possible for the molecule to have enough flexibility to achieve its biological functions (27).

Considering both the large size of the pocket and its tunnel nature, Chain A appears to contain a structure capable of accommodating ligands effectively. Thus, this region can be considered a good active site for molecular docking and virtual screening in search of antiviral drugs. Molecules that bind to this pocket can affect either receptor binding or induce conformational changes necessary for viral membrane fusion and therefore prevent infectivity of the rabies virus. It is known from earlier structural studies that the glycoprotein of the rabies virus contains sites necessary for receptor binding and immune recognition. Consequently, the found pocket and the tunnel system may be crucial elements responsible for these processes and suitable targets for designing novel antivirals and vaccines.

Pharmacophore property of ligands

The pharmacophoric features of Ribavirin were 13, including 1 aromatic, 4 hydrogen-bond donors, 7 hydrogen-bond acceptors and 1 hydrophobic feature (Fig. 7a). The abundance of H-bond acceptor and donor features may be important for molecular recognition and binding via hydrogen bonding interactions. Lauramide was found to have a pharmacophore profile dominated by hydrophobic components and two aromatic and two hydrogen-bond-accepting functional groups (Fig. 7b). Hydrophobic features are widespread and hydrophobic interactions might be important for molecular recognition and binding. N-dl-Alanylglycine exhibited 8 pharmacophore features, which included 2 hydrogen-bond donors, 4 hydrogen-bond acceptors, 1 negative ion and 1 hydrophobic feature (Fig. 7c). The high number of hydrogen-bond acceptor and donor features indicates the possible importance of hydrogen-bonding interactions in its molecular recognition and binding process. In addition, the RondonQSAR examination showed that lauramide had the highest predicted pEC50 (8.6718) and lowest EC50 (0.0021 µM), whereas Ribavirin demonstrated a pEC50 of 2.8730 and EC50 of 1339.6214 µM. N-dl-Alanylglycine has an extreme predicted value and should be interpreted cautiously. These QSAR predictions require further experimental validation (Table 5).

Anti-rabies activity *in silico* molecular docking of phytocompounds from *S. nigrum*

The molecular docking analysis of phytocompounds derived from the GC–MS profile of *S. nigrum* on the rabies viral protein revealed that the compounds, N-(2-phenylethyl)-N-methyl-lauramide, have shown significant interactions with the glycoprotein, which plays an essential role in cell adhesion and fusion. Lauramide G chain interaction represents GLU G : 45 forms a dominant anchor by engaging in multiple hydrogen bonds along with ASP G : 211 and ARG G:213, with a binding affinity of -4.81 kcal/mol (Fig. 8a, Table 6). The interaction with A chain exhibits good binding interactions by hydrogen bonding with Gln39 and 1038 residues, besides alkyl interaction with pro 41 and Val 89 with docking score -5.583 kcal/mol (Fig. 8b). On the other hand, N-dl-Alanylglycine docking with G chain interactions represents 3 hydrogen bond anchored by GLU: 45 with N terminal amine and addition hydrogen bonds with Tyr 43 and Asp 86, Trp240, Leu46, carbon hydrogen bond Lys217 and Thr239 (Fig. 9a, 9b). The docking score for N-dl-Alanylglycine was -4.86kcal/mol slightly inferior to that of lauramide. In Chain A, alanylglycine showed a predominantly hydrophilic cavity and five conventional hydrogen bonds with ASP99, SER100, SER98 and GLY100 and TYR52, along with core electrostatic interactions and the affinity was -4.7 kacal/mol (Fig. 9b, Table 7). Alanylglycine shows a more consistent docking pose, with root mean square deviation (RMSD) values (2.259/2.764 Å) that are much closer to each other, whereas lauramide has a large upper-bound RMSD of 6.331 Å. The Ribavirin binding affinities are −5.5 kcal/mol and −6.3 kcal/mol with respect to rabies virus glycoprotein (RVGP) chains G and A respectively (Table 8). Binding affinity with chain G represents conventional hydrogen-bond interactions with ARG G : 241 and MET G : 236, along with π–sulfur and alkyl interactions (Fig. 10a). The interactions with chain A were more favourable, with higher binding affinity and lower RMSD values indicating greater stability of the docked complex. Ribavirin has hydrogen-bond interactions with GLU46, TRP47, ASN60, ASP1001 and SER62, together with additional carbon-hydrogen interactions involving LEU45, LEU106 and MET1004, suggesting moderate binding towards both RVGP A chains with preference for chain A (Fig. 10b). The interaction of compounds derived from phytochemicals with the glycoprotein may affect receptor recognition or cause structural changes necessary for entry of many viruses into the host cell (28).

© The Author(s) 2026. Creative Commons CC BY 4.0. Published by Horizon e-Publishing Group.
https://doi.org/10.14719/pst.16217

Table 5. Comparative QSAR predicted pEC50 and EC50 among ligands

Parameter	Lauramide	N-dl-Alanylglycine	Ribavirin
D143	22.2658	12.1775	18.8265
D312	0.4199	1.0985	1.9383
D470	0.8595	0.0000	0.9680
pEC50	8.6718	−71.8510	2.8730
EC50	0.0021 µM	7.096×10^{77} µM	1339.6214 µM

Table 6. Binding affinity of lauramide with the rabies virus glycoproteins chain (*PDB* 6TOU)

Chain	Center (X, Y, Z)	Energy (kcal/mol)	rmsd/lb (Å)	rmsd/ub (Å)	Hydrogen bond	Other
G	13, -35, 4	-4.81	1.663	6.331	Arg, Glu, Asp	HP : Lys, Glu, Thr
A	-8, -12, -30	-5.583	1.144	2.033	Gln (2)	HP : Lys, Gln, Thr Pro, Val,

HP : hydrophobic.

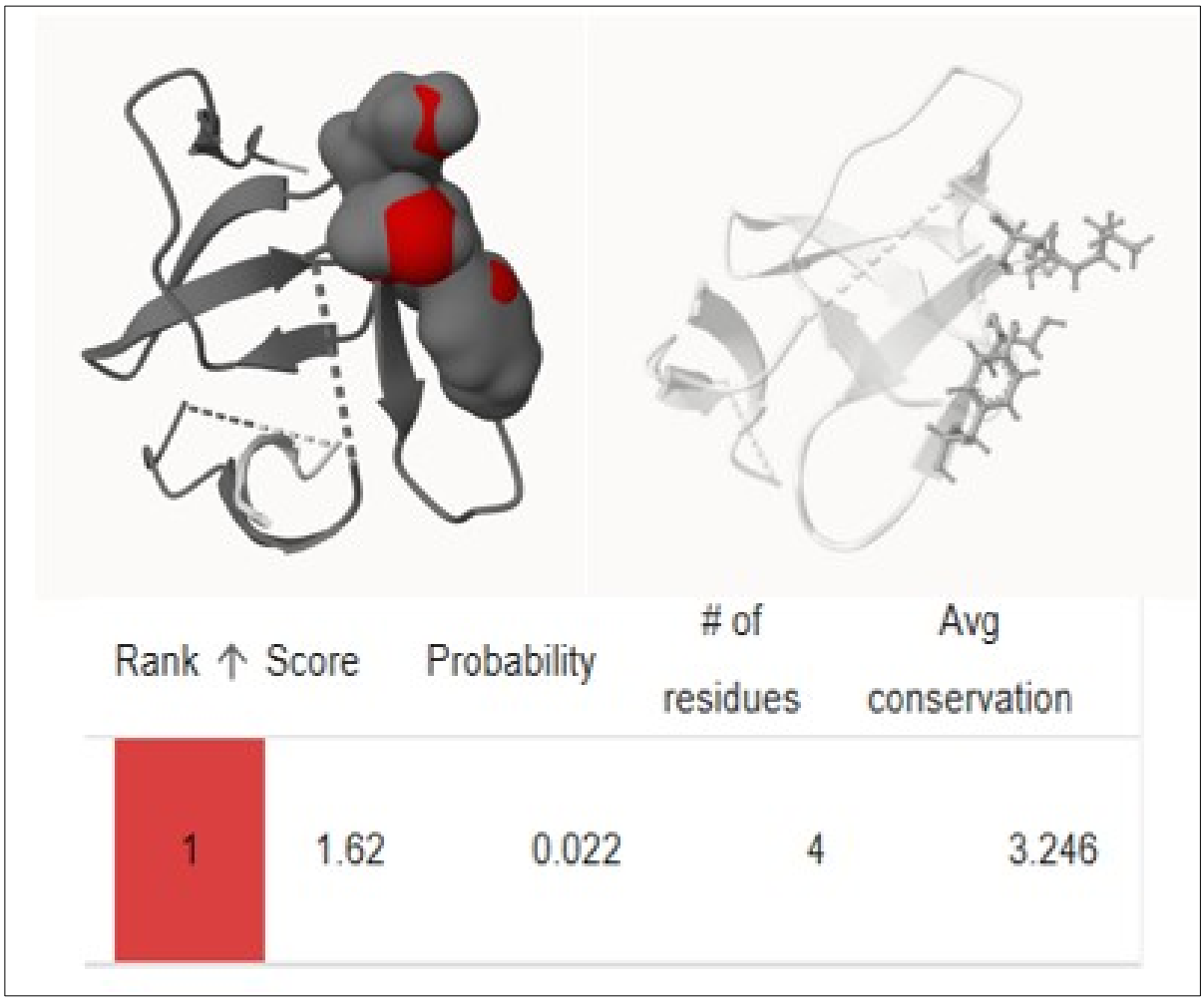
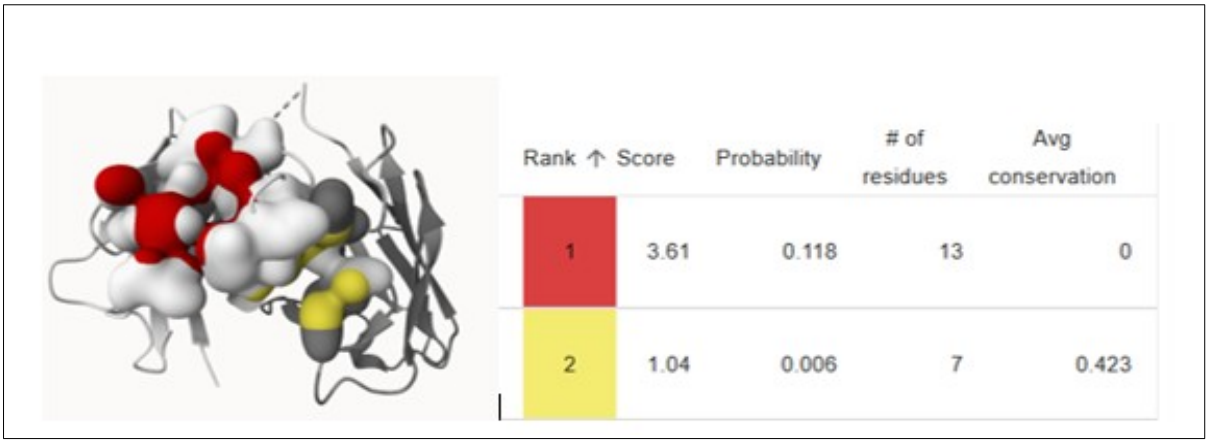


Fig. 5a. Pockets and tunnel analysed on rabies glycoprotein G chain (volume 65.4 Å³).

© The Author(s) 2026. Creative Commons CC BY 4.0. Published by Horizon e-Publishing Group.
https://doi.org/10.14719/pst.16217



Rank ↑	Score	Probability	# of residues	Avg conservation
1	3.61	0.118	13	0
2	1.04	0.006	7	0.423

Fig. 6a. Pockets analysed on rabies glycoprotein A chain (volume 565.1 Å³).



ID	Length (Å)	Min R (Å)	Avg R (Å)
1	5.51	1.15	1.41

Fig. 6b. Tunnel analysed on rabies glycoprotein A chain.

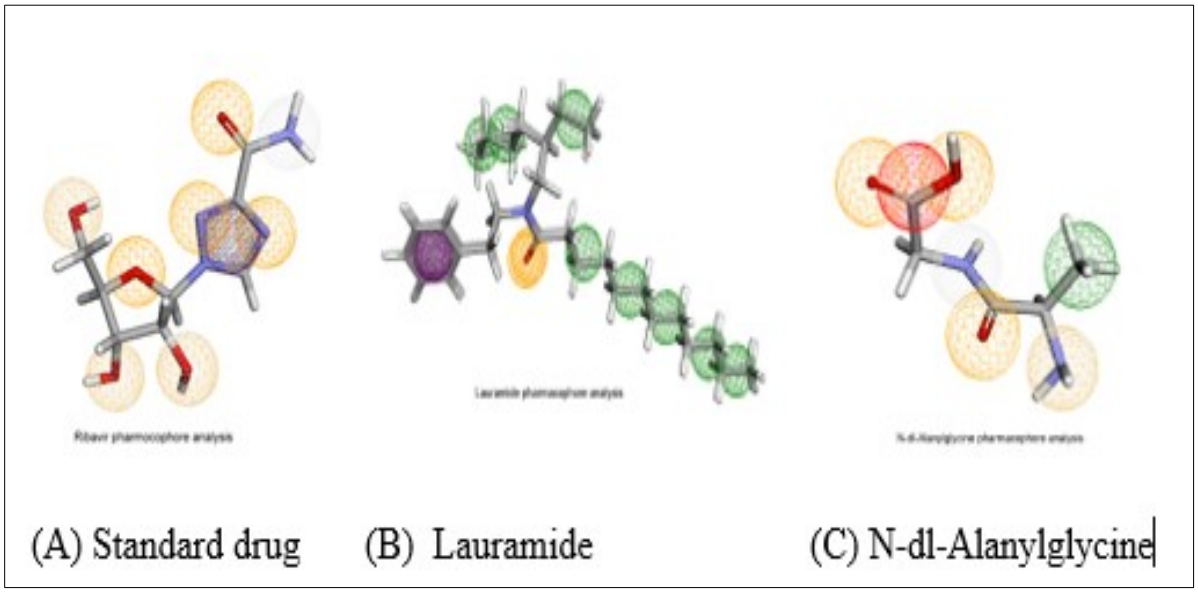


Fig. 7. Hydrogen bond donor and acceptor region of selected ligands.

© The Author(s) 2026. Creative Commons CC BY 4.0. Published by Horizon e-Publishing Group.
https://doi.org/10.14719/pst.16217

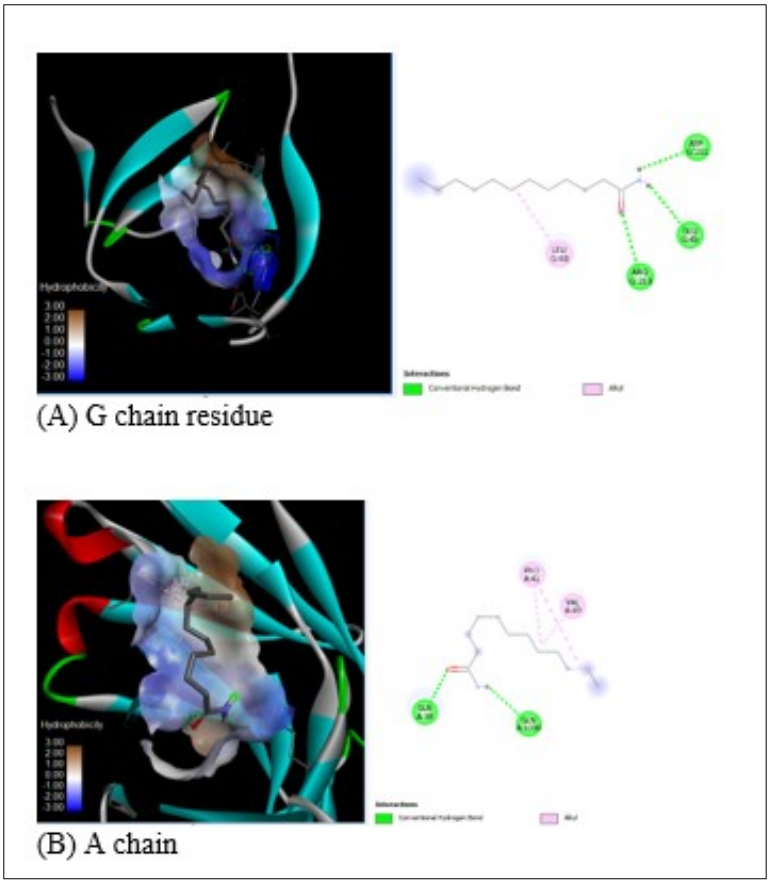


Fig. 8. Molecular interaction of selected ligand lauramide with rabies virus glycoprotein.

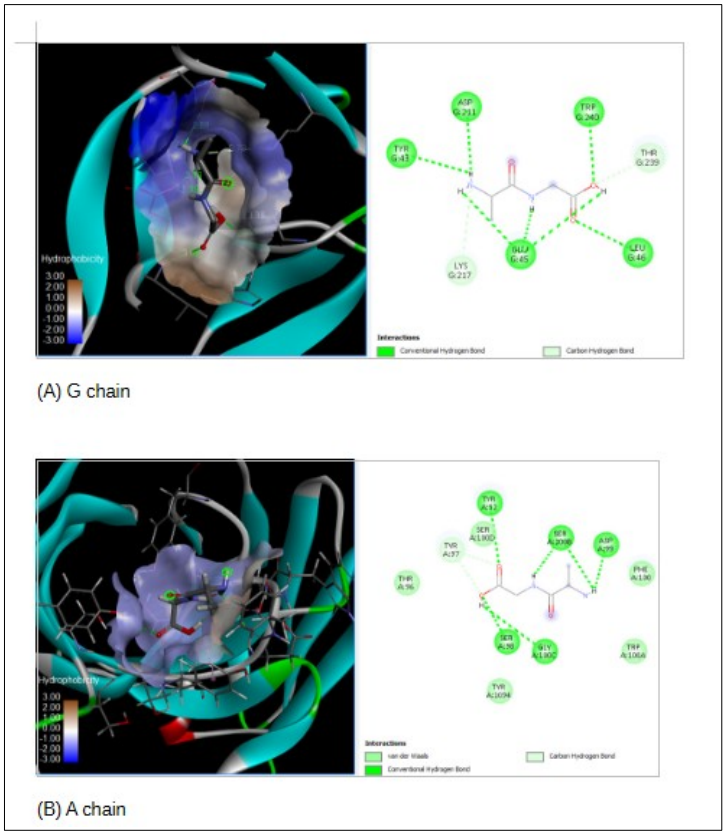


Fig. 9. Interaction of N-dl-Alanylglycine with rabies virus glycoprotein.

© The Author(s) 2026. Creative Commons CC BY 4.0. Published by Horizon e-Publishing Group.
https://doi.org/10.14719/pst.16217

Table 7. Binding affinity of N-dl-Alanylglycine with rabies virus glycoprotein chain (*PDB* 6TOU)

Chain	Center (X, Y, Z)	Energy (kcal/mol)	rmsd/lb (Å)	rmsd/ub (Å)	Hydrogen bond	Other
G	2, -39, -2	-4.86	5.603	6.931	Tyr, Asp, Glu,Trp, Leu	Leu Thr and Lys
A	1, -15, -20	-4.7	2.259	2.764	Ser (2), Gly, Asp, Trp, tyr,	Thr,Phe, Trp,Ser

Table 8. Binding affinity of standard drug with rabies virus glycoprotein (*PDB* 6TOU)

chain	Grid coordinates (x, y, z)	Binding affinity (kcal/mol)	RMSD l.b. (Å)	RMSD u.b. (Å)	Interacting residues	Hydrogen-bonding residues
G	(13, −35, 4)	−5.5	3.624	4.328	Cys, Arg, Asp	Cys, Met (weak)
A	(1, −15, −20)	−6.3	1.878	2.462	Asn, Gln	Gln, Thr, Gly, Met, Phe (weak)

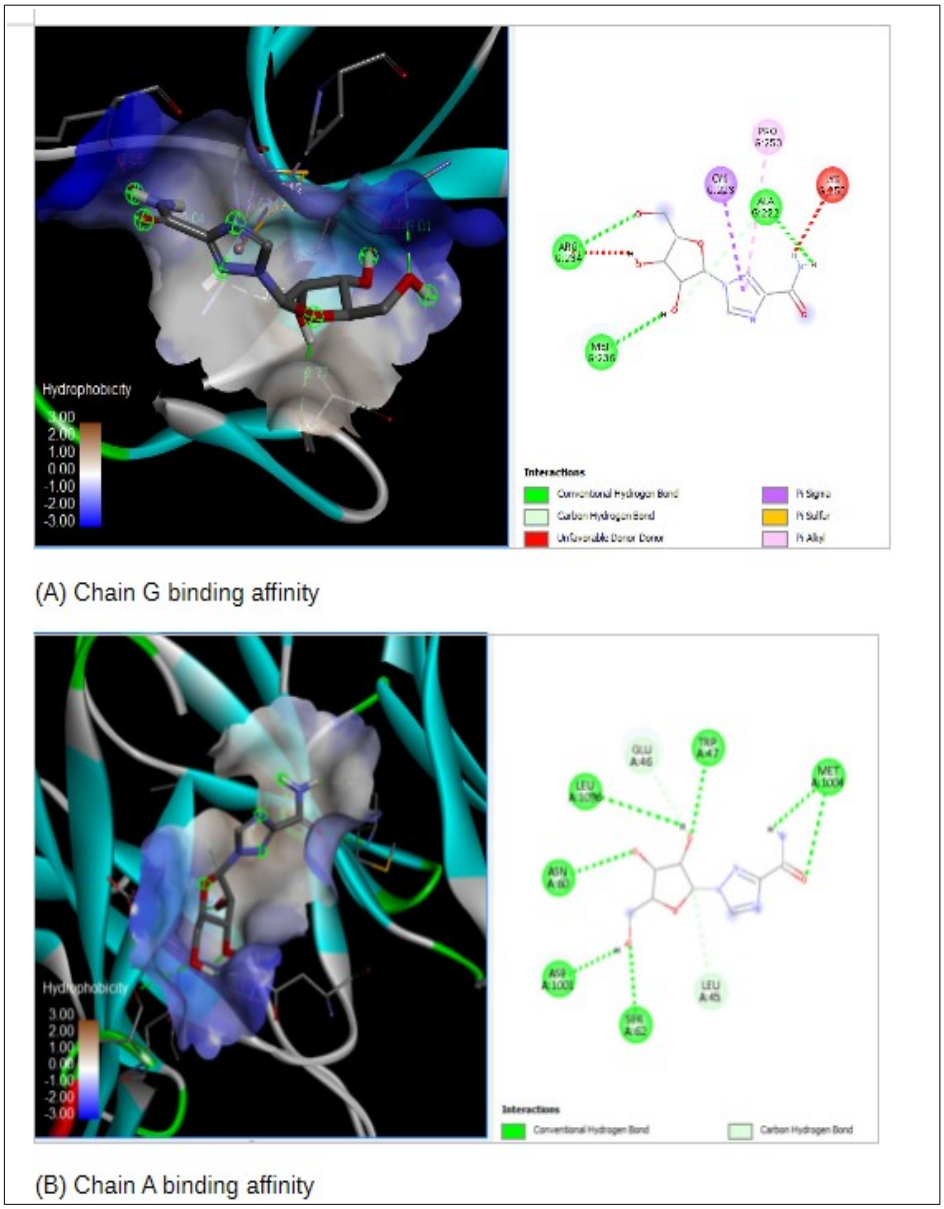


Fig 10. Interaction of ribavirin standard with rabies glycoprotein.

© The Author(s) 2026. Creative Commons CC BY 4.0. Published by Horizon e-Publishing Group.
https://doi.org/10.14719/pst.16217

Ribavirin is a broad-spectrum antiviral nucleoside analogue with activity against a wide variety of RNA and DNA viruses. Ribavirin remains an important therapeutic agent in various viral infections, but its potential against rabies has not been extensively explored (29). Hence, the predicted binding affinity of the phytocompounds was less effective than that of the standard antiviral ribavirin. Its blood–brain barrier (BBB)/central nervous system (CNS) permeability, which is higher than the standard, is an advantage for therapeutic application. The results suggest a potential molecular mechanism of phytochemicals' interaction with rabies drug targets; however, it requires post-experimental validation to confirm antiviral efficacy.

The structural analysis emphasised the role of conserved tyrosine and threonine residues in stabilising glycoproteins. Moreover, with the aid of computational methods, neutralising these residues was discovered to bind to RVG and inhibit membrane fusion (30). Lauramide has a better binding affinity due to the presence of the hydrophobic aliphatic chain and the aromatic group. According to previous research, hydrophobic interactions, along with hydrogen bonds, are critical for the stabilisation of glycoprotein-ligand complexes. Therefore, it can be concluded from the current study that lauramide is a more promising drug against rabies than N-dl-Alanylglycine. Most recently, the phytocompound morusinol was reported as a crucial therapeutic agent that blocks glycoprotein (G) (31). Compounds like epicatechin and cianidanol exhibit better binding affinity in contrast to our results and gallocatechin activity strongly supports the anti-viral phytochemical activity of medicinal plants (32).

Conclusion

The study revealed the ability of *Solanum nigrum* to be a good source of phytochemicals that possess significant biological activities in terms of antioxidant and anti-inflammatory properties. Selected bioactive compounds like lauramide and N-dl-Alanylglycine were found to interact with rabies virus glycoproteins. However, the results were weaker than those of standard drugs and may demand further intracellular investigations. Molecular dynamics simulations are additionally required to confirm the structural integrity of these protein-ligand complexes in physiological conditions. Together, these results provide a strong theoretical basis for creating affordable and sustainable anti-rabies strategies, outlining a clear path for future *in vitro* and *in vivo* experimental confirmation.

Acknowledgements

The authors would like to thank the management for providing the necessary facilities to carry out the work.

Authors' contributions

PDP carried out the *in vitro* studies and drafted the manuscript. NPMT acted as the research advisor and carried out the manuscript corrections. Both the authors read and approved the final manuscript.

Compliance with ethical standards

Conflict of interest

Authors do not have any conflict of interests to declare.

Ethical issues

None

Declaration of generative AI and AI-assisted technologies in the writing process

During the preparation of this work, the authors used auto dock prank web to perform molecular docking. After using this tool, the authors reviewed and edited the content as needed and take full responsibility for the content of the publication.

References

1. Admasu P, Deressa A, Mengistu A, Gebrewold G, Fayera T. In vivo antirabies activity evaluation of hydroethanolic extract of roots and leaves of *Phytolacca dodecandra*. Glob Vet. 2014;12(1):12–8. https://doi.org/10.5829/idosi.gv.2014.12.01.81150
2. World Health Organisation. Regional strategy for traditional medicine in the Western Pacific. Geneva: World Health Organisation; 2002.
3. Takayama N. Rabies: a preventable but incurable disease. J Infect Chemother. 2008;14(1):8–14. https://doi.org/10.1007/s10156-007-0573-0
4. Tahmasbi SF, Revell MA, Tahmasebi N. Herbal medication to enhance or modulate viral infections. Nurs Clin North Am. 2021;56(1):79–89. https://doi.org/10.1016/j.cnur.2020.10.007
5. Xiang L, Wang Y, Yi X, He X. Anti-inflammatory steroidal glycosides from the berries of *Solanum nigrum* L. (European black nightshade). Phytochemistry. 2018;148:87–96. https://doi.org/10.1016/j.phytochem.2018.01.019
6. Kaunda JS, Zhang YJ. The genus *Solanum*: an ethnopharmacological, phytochemical and biological properties review. Nat Prod Bioprospect. 2019;9(2):77–137. https://doi.org/10.1007/s13659-019-0201-6
7. Yang MY, Hung CH, Chang CH, Tseng TH, Wang CJ. *Solanum nigrum* suppress angiogenesis-mediated tumour growth through inhibition of the AKT/mTOR pathway. Am J Chin Med. 2016;44(6):1273–88. https://doi.org/10.1142/S0192415X16500713
8. Ye LF, Gao ZW. Study of *Solanum nigrum* n-butanol extract on the proliferation of human colorectal cancer SW480 and its mechanism. World J Integr Tradit West Med. 2019;14(3):356–8. https://doi.org/10.13935/j.cnki.sjzx.190315
9. Saranya P, Aarthi TS, Kalaivani D. Phytochemical analysis and pharmacological properties of *Solanum melongena* (L.) peel extracts: a potential source of natural therapeutic agents. Vegetos. 2025. https://doi.org/10.1007/s42535-025-01423-7

© The Author(s) 2026. Creative Commons CC BY 4.0. Published by Horizon e-Publishing Group.
https://doi.org/10.14719/pst.16217

10. Meyer RS, Whitaker BD, Little DP, Wu SB, Kennelly EJ, Long CL, et al. Parallel reductions in phenolic constituents resulting from the domestication of eggplant. Phytochemistry. 2015;115:194–206. https://doi.org/10.1016/j.phytochem.2015.02.006
11. Tunwagun DA, Akinyemi OA, Ayoade TE, Oyelere SF. Qualitative analysis of the phytochemical contents of different anatomical parts of ripe *Solanum aethiopicum* Linneaus fruits. J Complement Altern Med Res. 2020;9(3):14–22. https://doi.org/10.9734/jocamr/2020/v9i330142
12. Campisi A, Acquaviva R, Raciti G, Duro A, Rizzo M, Santagati NA. Antioxidant activities of *Solanum nigrum* L. leaf extracts determined in in vitro cellular models. Foods. 2019;8(2):63. https://doi.org/10.3390/foods8020063
13. Rahman H, Rahman N, Haris M, Mahmood R. Antioxidant and anti-inflammatory potentials of *Solanum pubescens* Willd an ethnomedicinal plant of South Western Andhra Pradesh, India. J Res Pharm. 2025;23(2):187–97.
14. Tomar NR, Singh V, Marla SS, Chandra R, Kumar R, Kumar A. Molecular docking studies with rabies virus glycoprotein to design viral therapeutics. Indian J Pharm Sci. 2010;72(4):486–90. https://doi.org/10.4103/0250-474X.73905
15. Jamal A, Nawaz A, Arif A, Shahid MN. Phytochemical and pharmacological potential of *Solanum nigrum*: a concise review. Acta Biol Slov. 2025;68(3):142–60. https://doi.org/10.14720/abs.68.3.20074
16. Roshan K, Mona K, Rupali H, Milind U. A review of the phytochemistry and pharmacological activities of Solanaceae family. Int J Pharm Chem Res. 2020;2(1):13–9. https://doi.org/10.33545/2664763X.2020.v2.i1a.15
17. Royani A, Mujawar NM, Hanafi M, Verma C, Lotulung PDN, Prastya ME, et al. Effect of solvent polarity on yield extract, antioxidant and antibacterial activities of phytochemicals from *Andrographis paniculata* leaves. Indian Chem Eng. 2025;67(1):1–15. https://doi.org/10.1080/00194506.2024.2409260
18. Zych M, Pyka-Pająk A. TLC in the analysis of plant material. Processes. 2025;13(11):3497. https://doi.org/10.3390/pr13113497
19. Sivakamasundari R, Mariajancyrani J, Chandramohan G. GC-MS analysis of chloroform extract of *Solanum nigrum* leaf. Sch Acad J Pharm. 2013;2(3):268–73. https://doi.org/10.36347/sajp
20. Rahman Lefta H. Biological activity of extract *Solanum nigrum* on some biological aspects of the blue fly *Chrysomya albiceps* (Diptera: Calliphoridae). Arch Razi Inst. 2022;77(3):1157–64. https://doi.org/10.22092/ARI.2022.357401.2038
21. Kulhade A, Shrivastava K. Identification of phytochemical compounds and their associated medicinal properties in *Solanum nigrum* fruit extract using gas chromatography–mass spectrometry. Libr Prog. 2024;44(6):603–10.
22. Sivaraj C, Yamini S, Yahavi A, Kumar RP, Arumugam P, Manimaaran A. Antioxidant, antimicrobial activities and GC-MS analysis of fruit extract of *Solanum nigrum* L. J Pharmacogn Phytochem. 2020;9(4):1114–21.
23. Zaidi SK, Ansari SA, Tabrez S, Naseer MI, Shahwan MJ, Banu N, et al. Antioxidant potential of *Solanum nigrum* aqueous leaves extract in modulating restraint stress-induced changes in rat's liver. J Pharm Bioallied Sci. 2019;11(1):60–8.https://doi.org/10.4103/jpbs.JPBS_58_18
24. Chen X, Dai X, Liu Y, Yang Y, Yuan L, He X, et al. *Solanum nigrum* Linn.: an insight into current research on traditional uses, phytochemistry and pharmacology. Front Pharmacol. 2022;13:918071. https://doi.org/10.3389/fphar.2022.918071
25. Yang F, Lin S, Ye F, Yang J, Qi J, Chen Z, et al. Structural analysis of rabies virus glycoprotein reveals pH-dependent conformational changes and interactions with a neutralizing antibody. Cell Host Microbe. 2020;27(3):441–53.e7. https://doi.org/10.1016/j.chom.2019.12.012
26. Hellert J, Buchrieser J, Larrous F, Minola A, de Melo GD, Soriaga L, et al. Structure of the prefusion-locking broadly neutralising antibody RVC20 bound to the rabies virus glycoprotein. Nat Commun. 2020;11(1):596. https://doi.org/10.1038/s41467-020-14398-7
27. Kokh DB, Amaral M, Bomke J, Grädler U, Musil D, Buchstaller HP, et al. Estimation of drug-target residence times by τ-random acceleration molecular dynamics simulations. J Chem Theory Comput. 2018;14(7):3859–69. https://doi.org/10.1021/acs.jctc.8b00230
28. Jabeen J, Ahmed N, Shahzad Z, Shahid M, Ahmad T. Insights for future pharmacology: exploring phytochemicals as potential inhibitors targeting SARS-CoV-2 papain-like protease. Future Pharmacol. 2024;4(3):510–40.https://doi.org/10.3390/futurepharmacol4030029
29. Hamran S, Al-Rajhi AA, Jasim K, Al-Theyab MA, Elahtam M, Al-Hail MK, et al. Efficacy and safety of adding ribavirin to sofosbuvir-based direct-acting antivirals (DAAs) in re-treating non-genotype 1 hepatitis C—a systematic review and meta-analysis. Diseases. 2025;13(5):138. https://doi.org/10.3390/diseases13050138
30. Lu Y, Cheng L, Liu J. Optimisation of inhibitory peptides targeting phosphoprotein of rabies virus. Int J Pept Res Ther. 2020;26(2):1043–9. https://doi.org/10.1007/s10989-019-09906-3
31. Li H, Habib O, Usman M, Usmani SA, Shafiq A, Akbar R, et al. In silico drug design targeting the rabies virus glycoprotein: phytochemicals as promising drug candidates. ChemistrySelect.2025;10(46). https://doi.org/10.1002/slct.202504329
32. Oranu EC, Ezeagha CC, Madueke AJ, Otarigho BE, Orjiakor J, Etuka IK. Molecular docking and virtual screening of *Boswellia dalzielii* phytochemicals as potential inhibitors of Rabies lyssavirus. GSC Biol Pharm Sci. 2025;33(2):267–79. https://doi.org/10.30574/gscbps.2025.33.2.0447

Additional information

Peer review: Publisher thanks the Sectional Editor and anonymous reviewers for their contribution to the peer review of this work.

Reprints & permissions information: Available at https://horizonepublishing.com/journals/index.php/PST/open_access_policy.

Publisher's Note: Horizon e-Publishing Group remains neutral with regard to jurisdictional claims in published maps and institutional affiliations.

Indexing: See https://horizonepublishing.com/journals/index.php/PST/indexing_abstracting.

Copyright: © The Author(s). This is an open-access article distributed under the Creative Commons Attribution License CC BY 4.0.

Publisher information: Plant Science Today is published by Horizon e-Publishing Group with support from Empirion Publishers Private Limited, Thiruvananthapuram, India.

© The Author(s) 2026. Creative Commons CC BY 4.0. Published by Horizon e-Publishing Group.

https://doi.org/10.14719/pst.16217